

Hydroxyapatite-Bioceramic/Expanded Perlite Hybrid Composites Coating on Ti₆Al₄V by Hydrothermal Method and in vitro Behavior

Mehtap Muratoğlu¹ and Tuğçe Özcan

Department of Metallurgy and Materials Engineering, Firat University, Elazığ, Turkey.

Biomedical Engineering and
Computational Biology
Volume 14: 1–12
© The Author(s) 2023
Article reuse guidelines:
sagepub.com/journals-permissions
DOI: 10.1177/11795972231151348



ABSTRACT: This study was aimed to coat a hybrid bioceramic composite onto Ti₆Al₄V by using hydrothermal method. The Hybrid bioceramic composite for coating was prepared by reinforcing different ratios of expanded perlite (EP) and 5 wt.% chitosan into synthesized Hydroxyapatite (HA). Coating was performed at 1800°C for 12 hours. The coated specimens were gradually subjected to a sintering at 6000°C for 1 hour. For in vitro analysis, the specimens were kept in Ringer's solution for 1, 10, and 25 days. All specimens were examined by SEM, EDX, FTIR, and surface roughness analyses for characterizing. It was concluded that as the reinforcement ratio increased, there was an increase in coating thickness and surface roughness. The optimum reinforcement ratio for expanded perlite can be 10 wt.% (A3-B3). With increasing ratio of calcium (Ca) and phosphate (P) (Ca/P), the surface becomes more active in body fluid and then observed the formation of the hydroxycarbonate apatite (HCA) layer. As the waiting time increased, there was an increase in the formation of an apatite structure.

KEYWORDS: Expanded perlite, hydroxyapatite, bioceramics, hydrothermal method

RECEIVED: September 4, 2022. **ACCEPTED:** December 27, 2022.

TYPE: Original Research

FUNDING: The author(s) disclosed receipt of the following financial support for the research, authorship, and/or publication of this article: This study supported financially by the Firat University Scientific Research Projects Management unit (FUBAP) under MF.18.51 project number.

DECLARATION OF CONFLICTING INTERESTS: The author(s) declared no potential conflicts of interest with respect to the research, authorship, and/or publication of this article.

CORRESPONDING AUTHOR: Mehtap Muratoğlu, Department of Metallurgy and Materials Engineering, Firat University, Elazığ Center, Elazığ 23119, Turkey. Email: mehtug@firat.edu.tr

Introduction

Increase in the human population has directly caused developments in science and technology. Materials used in repairing tissue damages occurring as a result of accidents and injuries experienced by humans and produced and developed to help the functioning of the body are known as biomaterials. The most important property expected from a biomaterial is that it is biocompatible. That is, a biomaterial is expected to be compatible with the tissues surrounding it and not induce unwanted side effects on the tissue. This is why it is desired that every material used in the body is biocompatible.¹ Implants that are used as biomaterials are categorized as metallic, ceramic, polymer, and composite materials.²

Materials such as titanium and its alloys, cobalt and its alloys, stainless-steel, and gold are used as metallic biomaterials as they have high strength and wear resistance.^{3,4} Titanium and its alloys are preferred in several biomedical applications as they do not react with the oxygen in the air and do not form oxides, and they are durable. Additionally, due to the compatible structure of biomaterials made out of titanium and its alloys with bone, they are prevalently preferred for use.⁵⁻⁸ Hydroxyapatite (HA) is a biocompatible biomaterial that is usually used in coating bones, teeth, and implants. Hydroxyapatite (HA) [Ca₁₀(PO₄)₆(OH)₂] constitutes 70% of the bone structure. It is also preferred as it has high bioactivity and biodegradability and does not have any toxic effects.^{9,10} In recent years, in the fields of orthopedics and dental implants,¹¹ several studies have been carried out Hydroxyapatite (HA) coating to the metal implants (Ti, Ti₆Al₄V, 316 L stainless-steel).¹²

Various techniques have been developed to coat Hydroxyapatite (HA) onto the surfaces of titanium and its alloys. Examples of these may be listed as CVD (chemical vapor deposition), PVD (physical vapor deposition), plasma spray, vacuum plasma, HVOF (high-velocity oxygen fuel thermal spray process), sol-gel submersion, and EPD (electrophoretic coating). All of these methods have some disadvantages about the poor connection between coating and the surface.¹³ Plasma spray coating is the most frequently used method in uncemented hip prosthetic surgeries. However, plasma spray Hydroxyapatite (HA) coatings have some unwanted properties such as composition, structural control, and weak adhesive strength.¹⁴ The hydrothermal method that has recently been used as a coating method, was preferred in our study since its reaction temperature is lower than 200°C, process time is short, the coating is more homogenous, and the method is low-cost.¹⁵⁻¹⁸

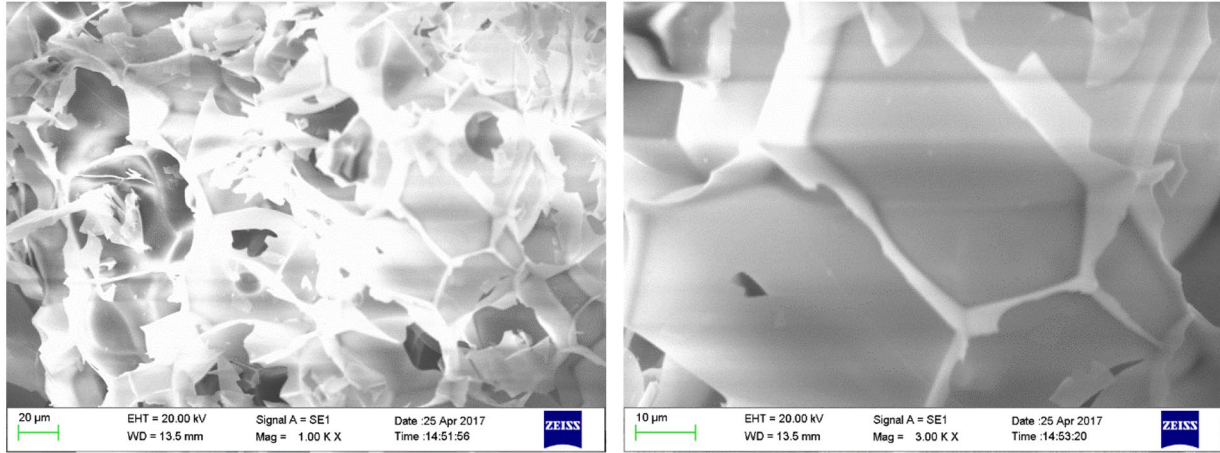
Studies with bioactive glasses have a significant place in the repair of damaged tissues. Bioactive glasses have high biocompatibility properties with the help of their composition consisting of SiO₂, Na₂O, CaO, and P₂O₅. This is because bioactive glass contains almost 60% SiO₂ and Na₂O, CaO, and P₂O₅ by weight in its composition, and these components become highly active in aqueous environments such as body fluids. Moreover, MgO and Al₂O₃, which may be found in the composition of bioactive glasses, can form a bond with body tissues.¹⁹⁻²¹ Also, chemical composition of the expanded perlite (EP) contains 60% to 75% SiO₂, 10% to 15% Al₂O₃ and with different ratio of K₂O, MgO, CaO, and Fe₂O₃. Considering this perspective, expanded perlite shows many similarities to



Creative Commons Non Commercial CC BY-NC: This article is distributed under the terms of the Creative Commons Attribution-NonCommercial 4.0 License (<https://creativecommons.org/licenses/by-nc/4.0/>) which permits non-commercial use, reproduction and distribution of the work without further permission provided the original work is attributed as specified on the SAGE and Open Access pages (<https://us.sagepub.com/en-us/nam/open-access-at-sage>).

Table 1. Chemical composition of Expanded perlite (EP) (in wt.%).

COMPOSITION	SiO ₂	Al ₂ O ₃	K ₂ O	MgO	CaO	Fe ₂ O ₃	Na ₂ O ₃	TiO ₂	MNO ₂	SO ₃
wt.%	74	14.33	4.95	0.28	0.5	0.97	2.9	0.12	0.07	0.03

**Figure 1.** SEM images of the Expanded perlite (EP).**Table 2.** The chemical composition of the Ti₆Al₄V alloy substrate.

C	FE	N	O	AL	V	H
<0.08	<0.25	<0.05	<0.02	5.5-6.76	3.5-4	<0.015

commercial inert glass, bioceramic glass and especially bioactive glass.^{22,23} chitosan is frequently used in tissue engineering due to its properties such as biocompatibility, bioactivity, and biodegradability.^{24,25} Furthermore, it supports cell adhesion and multiplication. Chitosan allows the formation of a porous scaffolding structure that supports the tissue scaffold. Due to these properties, it is prevalently used in studies conducted on Hydroxyapatite.²⁶

In this study, we aimed to coat a titanium alloy (Ti₆Al₄V) with Hydroxyapatite (HA)- Expanded Perlite (EP) and Hydroxyapatite (HA)- Expanded Perlite (EP)-Chitosan using by hydrothermal coating method. This method which has several superior aspects to the other researched coating methods was preferred in our study since its reaction temperature is lower than 200°C, process time is short, the coating is more homogenous, and the method is low-cost. Also, Expanded perlite was investigated with respect to its properties as component of composite systems considered for biomedical applications. chemical composition of the expanded perlite (EP) shows nearly same amount with biomaterials especially bioceramic glass. It has high reserve with low cost. Although the effect of perlite with different factors has been studied and observed in many field, there is a lack of knowledge of perlite at biocomposite materials, and still need for more research to be able to determine the optimum settings for the biocomposite coating in different HA-reinforcement combinations. In this respect, many advantages in terms of properties,

biocompatibility, as well as low cost could be ascribed to the realization of Expanded Perlite. In none of the previous studies, expanded perlite as a additives for the biomaterials have been subjected to this hydrothermal method in coating. So, it was targeted in this study to compare the coating thicknesses forming on the surfaces of the specimens, and the conditions in which the best coating obtained were examined according to the SEM-EDX, XRD, and FTIR results.

Materials and Methods

The expanded perlite used in the experiments was obtained from the firm of the Nanography (Nano technology informatics manufacturing and consulting C LLC. (Ankara, Turkey)). The size of expanded perlite is 50 microns, and the chemical composition of the expanded perlite is shown in Table 1. Also, Figure 1 shows the SEM images of the expanded perlite. The P₂O₅ and Ca(NO₃) used as the sources of Hydroxyapatite (HA) and the Ti₆Al₄V alloy used as a base material in the experiments were obtained from the firm of fytronix scientific instruments (Elazığ, Turkey).

Preparation of Ti₆Al₄V plates

The chemical composition of the Ti₆Al₄V alloy used as the base material in the experiments is shown in Table 2. The surfaces of the Ti₆Al₄V alloy material were grinded (400-1200 mesh). The surfaces of the specimens were then cleaned

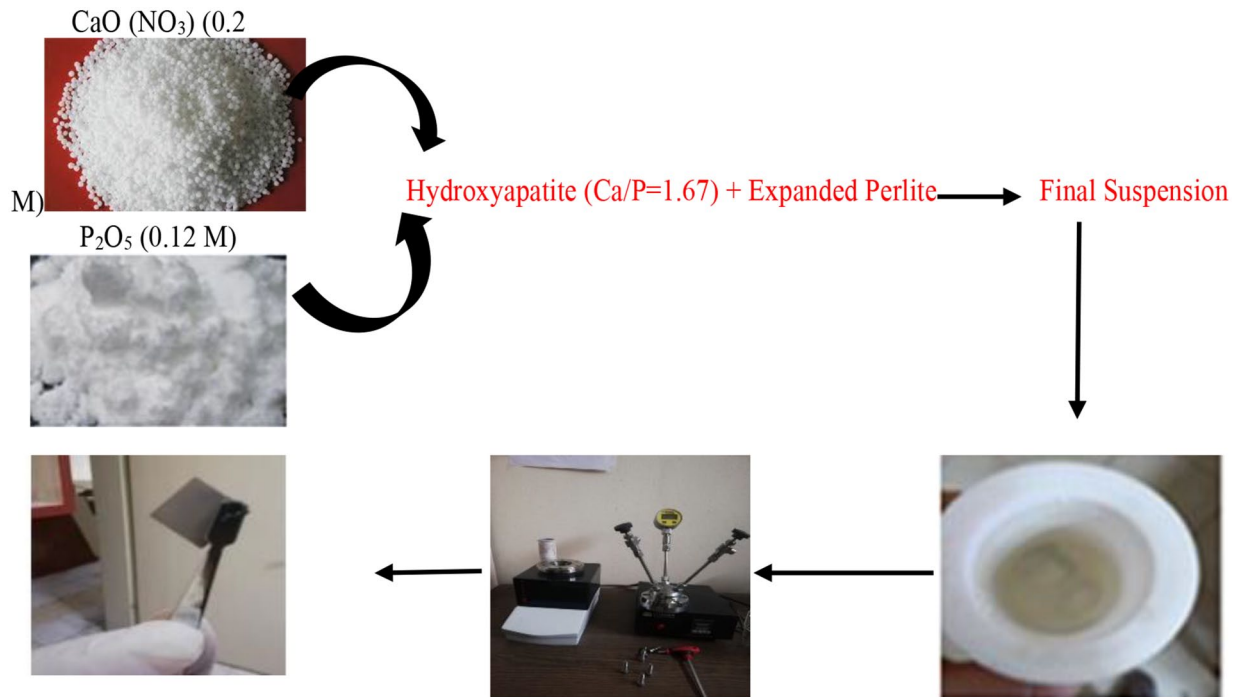


Figure 2. The schematic representation of the synthesis of hybrid coating on $\text{Ti}_6\text{Al}_4\text{V}$.

Table 3. The codes and contents of used specimens.

WITHOUT HEAT TREATMENTED (A)		HEAT TREATMENTED (B)	
A1	HA + %5EP	B1	HA + %5EP
A2	HA + %5EP + %5 Chitosan	B2	HA + %5EP + %5 Chitosan
A3	HA + %10EP	B3	HA + %10EP
A4	HA + %15EP	B4	HA + %15EP
A5	HA + %15EP + %5 Chitosan	B5	HA + %15EP + %5 Chitosan

with ethanol, acetone and distilled water. The cleaned specimens were kept in a 66.3% H_2SO_4 and 10.6% HCl solution at a weight ratio of 1:1 at 60°C for 1 hour. After the specimens were dried at room temperature, and a group of specimens was subjected to a preliminary heat treatment process at 600°C .

Preparation of coating solution

Calcium nitrate $\text{Ca(NO}_3\text{)}$ and di-phosphorus pentoxide (P_2O_5) were dissolved in 15 ml distilled water for Hydroxyapatite (HA) synthesis, so that the calcium (Ca) and phosphate (P) stoichiometric ratio would be 1.67 (Ca/P). The expanded perlite used at ratios of 5%, 10%, and 15% as a reinforcement material was dissolved in 15 ml distilled water. The obtained solutions were dissolved into each other on a magnetic stirrer. It was ensured that the solution on the magnetic stirrer had

10 pH by using NH_3 . The resulting solution and the $\text{Ti}_6\text{Al}_4\text{V}$ alloy were subjected to the coating process in a hydrothermal method (12 hours, 180°C). Figure 2 shows the steps of the hydrothermal process. The codes of the obtained specimens are presented in Table 3.

Characterization of synthesized hydroxyapatite coating

The characterizations of the hybrid coatings were carried out by scanning electron microscope attached to energy dispersive spectroscopy (SEM-EDS, Jeol, JSM-7001F), atomic force microscope (AFM, Park System 100-E), X-ray diffraction (XRD, Bruker D8), and Fourier-transform infrared spectroscopy (FTIR, Thermo Scientific™ Nicolet™ iS™5) spectroscopy. Also, the surface roughness of the specimens was measured using an SRT-6210 digital portable surface roughness Measurement device.

In vitro tests

In vitro tests were conducted to determine the biocompatibility of the biocomposite specimens. Ringer's lactate solution was used for the in vitro tests. Ringer's solution is frequently used in in vitro tests on organs or tissues and assessment of titanium coatings, and it resembles the chemical composition of human blood plasma to a large extent.²⁷⁻³⁰ The chemical compositions of Ringer's solution and human blood are presented in Table 4. For each coated specimens were kept in 75 ml Ringer's lactate solution at 37°C for 1, 10, and 25 days for the in vitro processes.

Table 4. Chemical composition of SBF and Ringer's solution.³¹

CONCENTRATION (MMOLL ⁻¹)		
ION	HUMAN BLOOD PLASMA	RINGER'S SOLUTION
Na ⁺	142	147.2
K ⁺	5	4
Mg ²⁺	1.5	-
Ca ²⁺	2.5	2,2
Cl ⁻	103	155.7
HCO ₃ ⁻	27	-
HPO ₄ ⁻	1	-
SO ₄ ²⁻	0.5	-

Experimental Results and Discussion

Micrography results

Figures 3 to 6 show the SEM images -EDX analysis of the coated A specimens.

It was observed that a connected and porous structure was present on the surface coatings of all A specimens, but there was no homogenous distribution. Lack of a homogenous distribution on the coating surface makes osteointegration easier.³² It is thought that the porous structure observed was caused by the structure of the expanded perlite and HA.³³ Morphology of the HA is rough and porous. These pores are called macro pores because of the pores diameter which it is bigger than 100 μm . Porosity increases the surface area and provides a broader area for bone cell growth.³⁴ A bioactive glass has a composition of 44.97% to 58.47% SiO₂, 17.79% to 24.49% CaO, 17.76% to 24.55% Na₂O, and 5.98% to 5.99% P₂O₅.³⁵ This glass was kept in simulated body fluid and formed a calcium phosphate layer. By conducting biological and toxicological tests on the obtained specimens, they supported their use in bone applications as they had high phosphate contents.³⁶ In addition to containing high amounts of Al₂O₃ and SiO₂ in its structure, expanded perlite also contains MgO, CaO, and Fe₂O₃. It also contains trace amounts of Na₂O, CaF₂, and P₂O₅. The component density observed in the EDX analysis (Figure 3) supported the contents of expanded perlite.

When the A1 and A2 specimens were compared in terms of chitosan reinforcement, it was observed that the coating thickness increased from approximately 4.863 to 9.902 μm . This was because chitosan supports cell adhesion and multiplication due to its chemical structure and allows the formation of internally connected pores that provide in vitro and in vivo bone tissue formation.³⁷

As shown in Figure 5, as the ratio of expanded perlite was increased, there were variable change in the coating thickness. While the coating thickness at the expanded perlite ratio of 5 wt.% was approximately 4.86 μm , it was observed to increase

approximately 2-fold (9.19 μm) when this ratio was increased to 10 wt.%. However, when the expanded perlite reinforcement ratio became 15 wt.%, the thickness was observed unexpectedly as 2.87 μm . This was the lowest coating thickness value that we obtained. While the reason for this is not completely known, we observed that reinforcement components have some limiting ratio that we encountered in some examples from the literature. A study about the limiting nature of reinforcement components was conducted by Demirkol et al produced composites by adding commercial inert glass to synthetic HA at ratios of 5 and 10 wt.%. They selected the temperature range of 1000°C to 1300°C to observe the effects of sintering. They observed better results in composites with the sintering temperature of 1300°C where 5 wt.% commercial inert glass was used.³⁸

In the comparison of the A4 and A5 specimens, it was observed that the thickness of coating increased more with the addition of chitosan when the expanded perlite ratio was 5 wt.%. This showed us that chitosan reinforcement increased thickness at low expanded perlite reinforcement ratios. When the A4 (2.87 μm) and A5 (6.76 μm) specimens were compared, it was seen that the thickness increased when chitosan was reinforced into the specimen with the lowest thickness obtained. These suggested that chitosan supports cell adhesion and multiplication.³⁹

Figures 7 to 10 show the SEM-EDX analysis of the B specimens. In the B group of specimens, a porous surface morphology with a low crack density and different zone were observed on the SEM images. This porous structure makes osteointegration easier in bioceramic-coated implants.³² The porous and rough nature of the obtained coating is an important factor in increasing bioactivity in addition to providing the use of bone-producing cells in these areas.³² While the macropore diameter may be greater than 100 μm , the micropore diameter may be smaller than 10 μm . Porous structures smaller than 1 μm play a role in bioactivity as they facilitate the interaction of proteins.⁴⁰ Additionally, for good adhesion between the coating and the metal, crack-free structures need to be obtained. If sufficient adhesion is achieved between the coating and the implant, coating-tissue interaction is achieved, and the implant is fixed onto the tissue. This means a faster and better integration of the implant to the tissue.⁴¹⁻⁴³ It is also thought that the dense structures observed in the EDX analysis originated from the content of HA and rich content of expanded perlite.

In the comparison of the B1 and B2 specimens, chitosan reinforcement into the coating under the same conditions and reinforcements by 5 wt.%, increased the coating thickness from 4.453 to 9.12 μm .

As seen in Figure 9, in the B specimen group, as the expanded perlite reinforcement increased, the coating thickness increased linearly. When the expanded perlite reinforcement ratio was 5%, the coating thickness was 4.453 μm . When the expanded perlite reinforcement ratios were 10% and 15%, the coating thicknesses became respectively 6.85 and 9.12 μm .

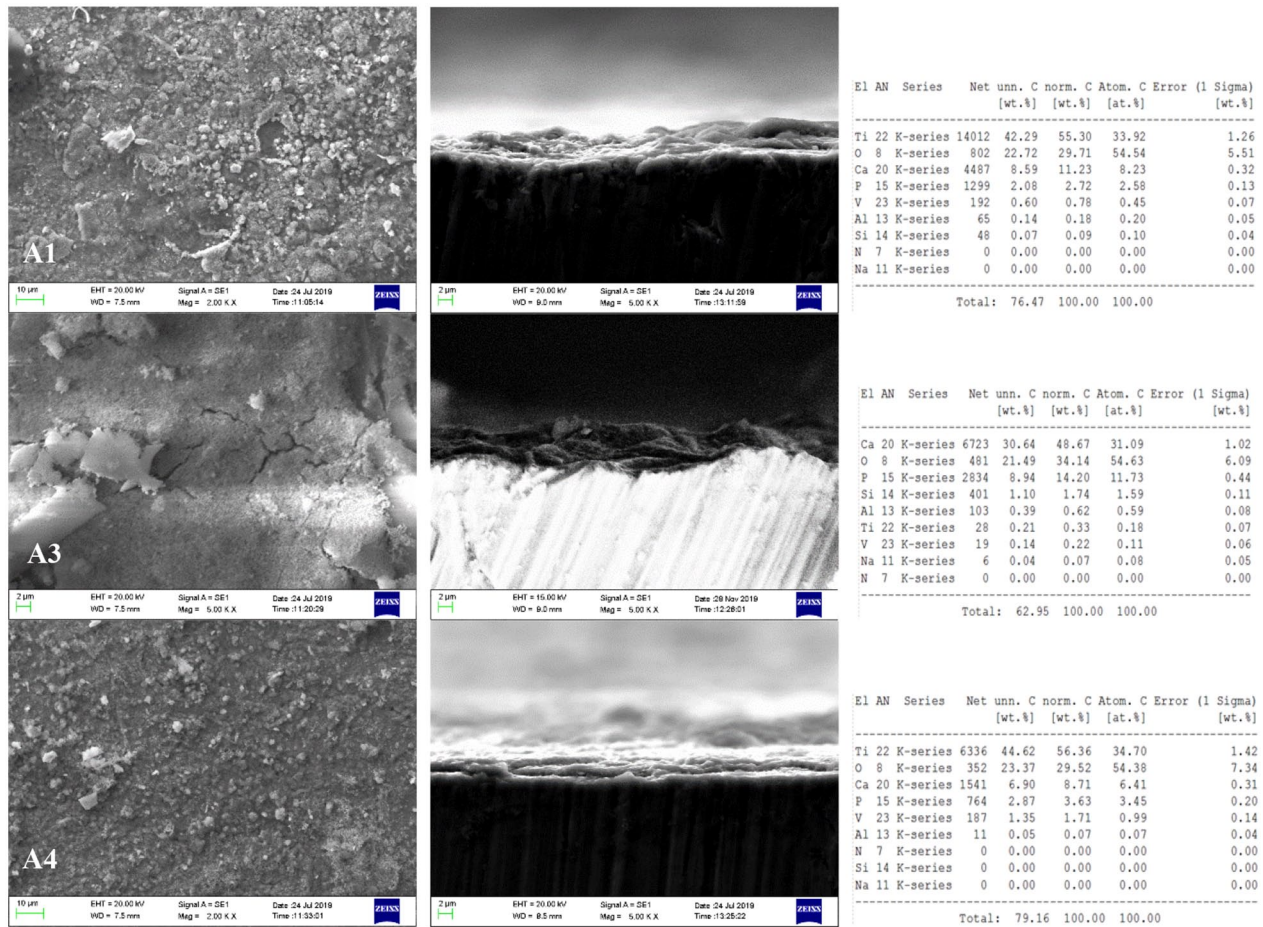


Figure 3. SEM images and EDX analysis of A1, A3, and A4 specimens with different magnifications.

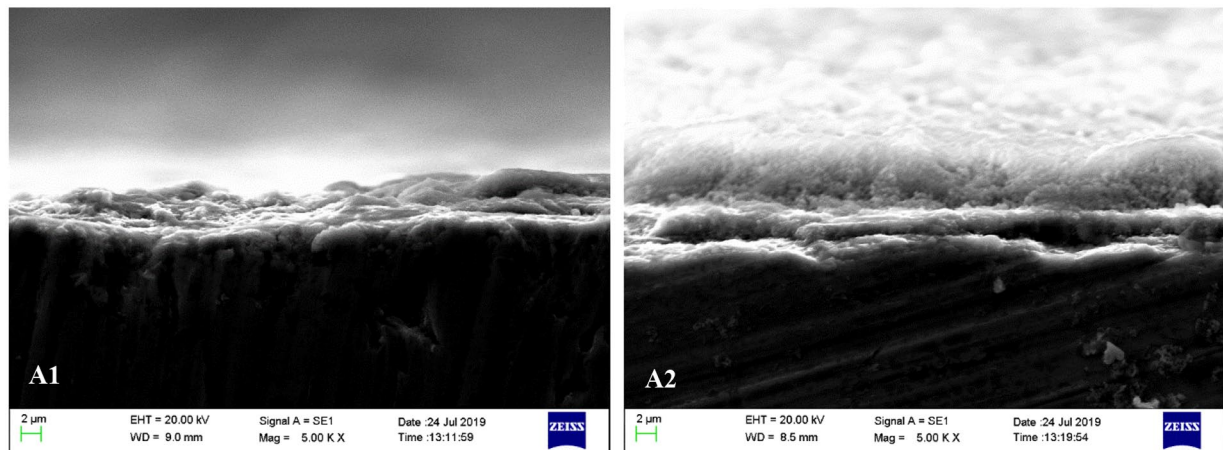


Figure 4. SEM images of cross-section of the hybrid coatings for A1 and A2 specimens.

The study by Say et al⁴² supported the results of our study. They observed that the adhesive strength of HA was lower than coating with HA-SiO₂. Other studies have also observed that adding silicate into the HA improved thermal stability, dissolvability and mechanical properties.⁴⁴⁻⁴⁶

As seen in Figure 10, when 5 wt.% chitosan was added to the 15 wt.% expanded perlite-reinforced specimens, the coating

thickness decreased from 13.89 to 9.43 μ m. That is, when B4 and B5 were compared, addition of 5 wt.% chitosan into 15 wt.% expanded perlite reinforcement reduced the coating thickness. Since the coatings will be in contact with the liquids in the human body, they will show wear behavior over time. Wear tests are also required to measure the wear behavior of the coatings and to calculate the friction coefficients. Work on this will continue.

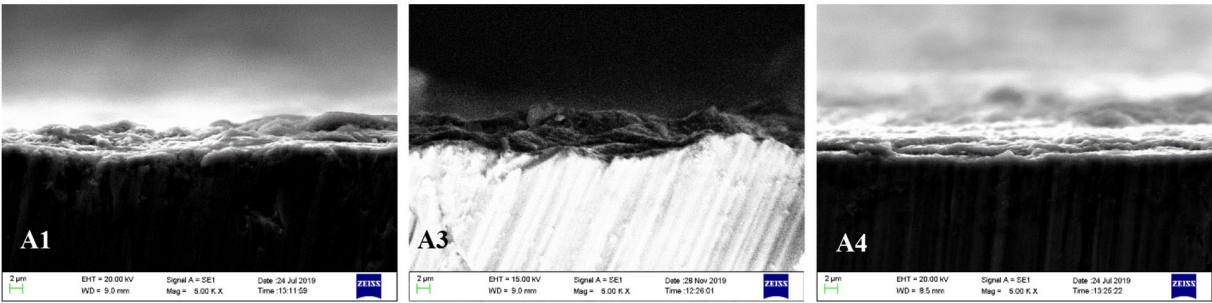


Figure 5. SEM images of cross-section of the synthesized hybrid coatings for A1, A3, and A4 specimens.

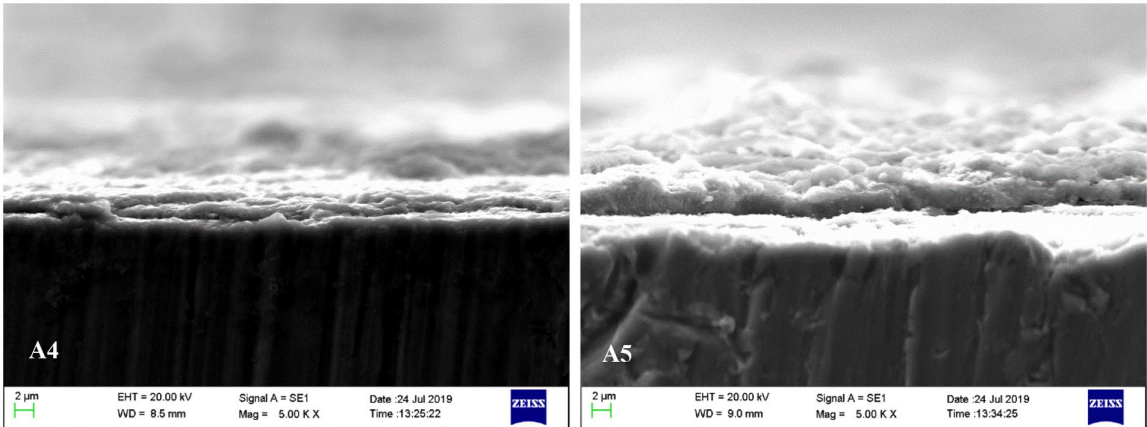


Figure 6. SEM images of cross-section of the synthesized hybrid coatings for A4 and A5 specimens.

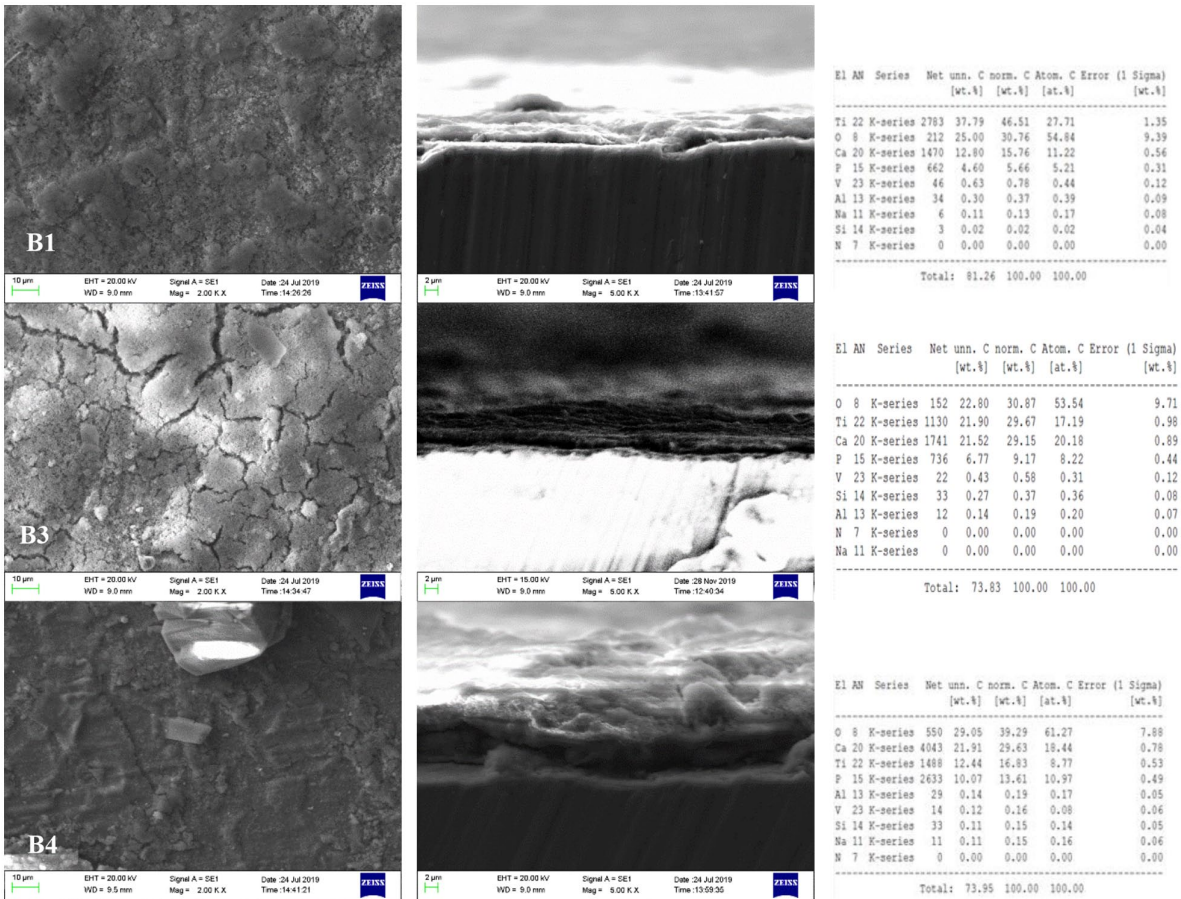


Figure 7. SEM images and EDX analysis with different magnifications for B1, B3, and B4 specimens.

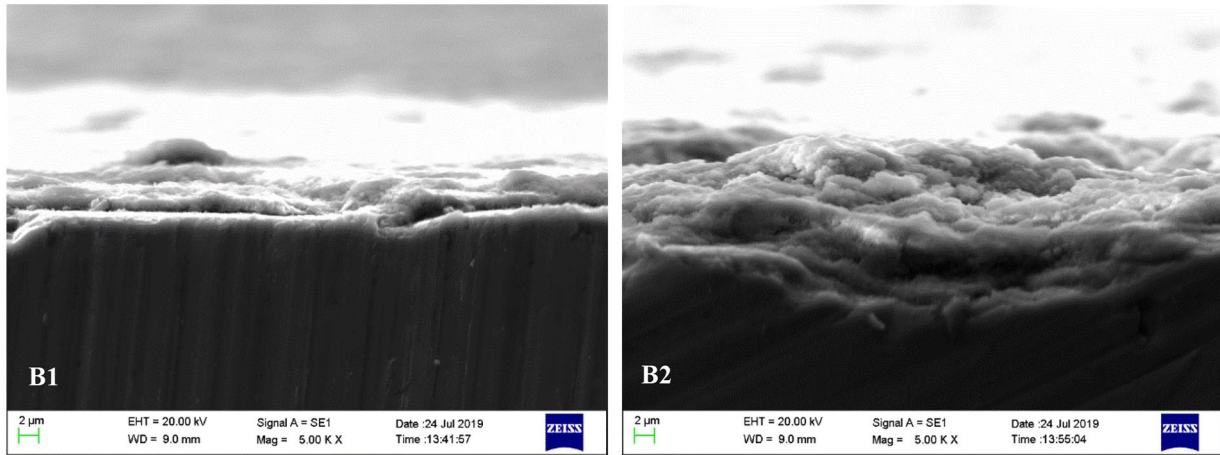


Figure 8. SEM images of cross-section of the hybrid coatings for B1 and B2 specimens.

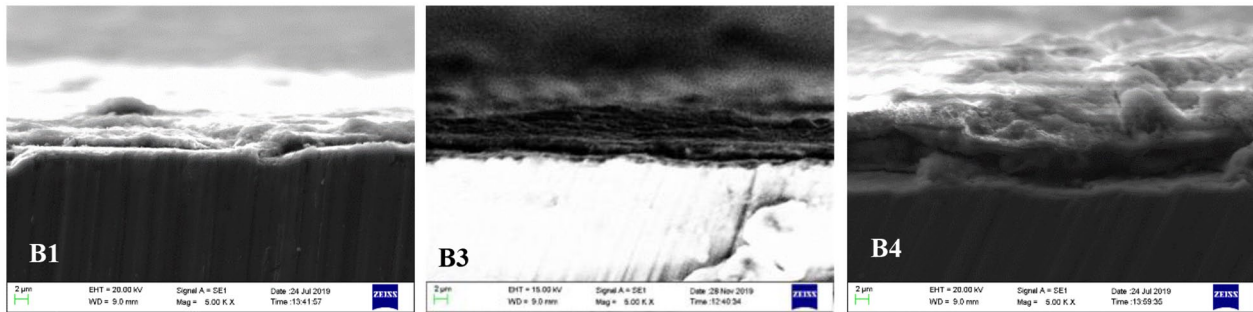


Figure 9. SEM images of cross-section of the hybrid coatings for B1, B3, and B4 specimens.

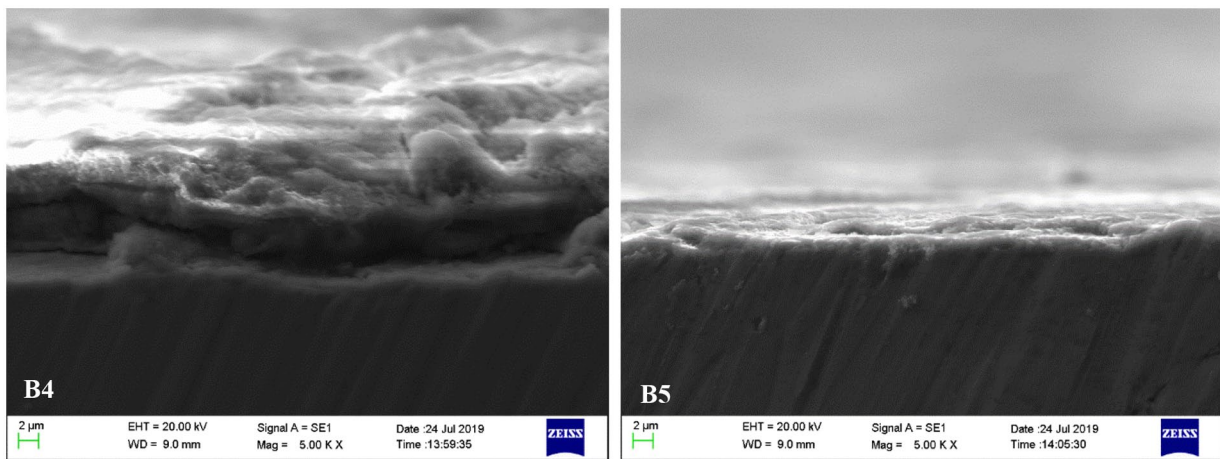


Figure 10. SEM images of cross-section of the hybrid coatings for B4 and B5 specimens.

X-ray analysis

The X-ray analysis of the B1 and B2 specimens are shown in Figure 11.

$\text{Ti}_6\text{Al}_4\text{V}$ and HA peaks were intensively observed in the XRD analyses of the B1 and B2 specimens. The P_2O_5 as the phosphate source and the $\text{Ca}(\text{NO}_3)_2$ used as the calcium source led to the formation of HA. The B2 specimen additionally contained 5 wt.% chitosan reinforcement in difference to the B1 specimen provided the same peak values. The reason for this

was that the structure of chitosan resembles naturally obtained HA. Chitosan is prevalently preferred in the world of medicine as it is biodegradable, non-toxic and has qualities like cell adhesion and minimal reaction with foreign bodies. It also supports bone formation in in vitro and in vivo environments due to its osteoconductive property. The polysaccharide scaffold structure of chitosan is similar to glycosaminoglycan that are the main extracellular matrix component of bone.^{47,48} This is why it is frequently preferred in tissue engineering. In addition to these

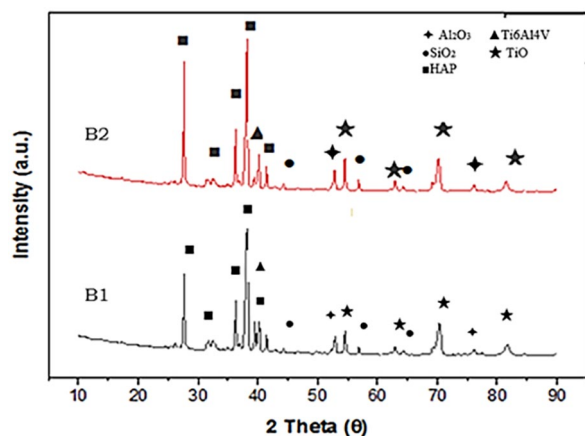


Figure 11. The X-ray diffraction (XRD) pattern of B1 and B2 specimens.

properties, as it cannot show a bioactive property by itself, it is used together with HA.^{49,50} Other peaks observed in the XRD analysis were TiO_2 , SiO_2 , and Al_2O_3 . The TiO_2 film that is formed creates an interface connection between the $\text{Ti}_6\text{Al}_4\text{V}$ base and the HA coating.⁵¹ It is thought that the formation of the TiO_2 structure originates from the oxidation of titanium atoms during the sintering process. It is considered that the SiO_2 and Al_2O_3 structures come from the contents of expanded perlite. This is because the content of expanded perlite includes high ratios of SiO_2 and Al_2O_3 .⁵² Al_2O_3 , which is bioinert, is frequently used in studies, usually by reinforcing into HA. It was determined that, when used alongside HA, Al_2O_3 increased hardness and strength.⁵³ Furthermore, it is frequently preferred in load-bearing hip prosthetics due to its good biocompatibility, corrosion resistance within body fluids and mechanical properties.⁵⁴ Moreover, the study by Li et al.⁵⁵ found that SiO_2 was a component of bioactive glass and had the capacity to form apatite in SBF. It was supported by the information in the literature that the peaks obtained within the scope of our study were also used in other studies on biocompatibility. This supported the usability of expanded perlite (EP) in the place of bioglass in studies where bioglass is used as a reinforcement, biocompatibility is desired.

In vitro analysis

The SEM images of the B1, B2, and B3 specimens kept in Ringer's solution for 1, 10, and 25 days were given in Figure 12. EDX analysis was conducted for the specimens kept in the solution for 10 days (Figure 12).

The SEM analyses shown in Figure 12 reveal highly porous and rough structures. The property of bioactive glasses and ceramics is formation of a hydroxycarbonate apatite (HCA) layer with collagen tissue fibers. For the formation of the HCA layer, calcium-based phosphates and silicates are highly important.^{56,57} The content of expanded perlite and the structures of bioactive glasses and ceramics are highly similar.⁵⁸ When Figure 11 is examined, it is seen that the HCA layer (white layers) was formed even after 1 day in the B2 and B4 specimens. The EDS

analyses revealed Ca, P, Mg, Na, O, and Si. Na ions were encountered in the EDX analysis of the specimens kept in the SBF (in vitro) solution. It is believed that this came from Ringer's solution. It is known that these elements, which show a very low toxic effect in the human body, have effects on bioactivity and biocompatibility.^{29,59}

The XRD analysis of the B2 specimen with and without in vitro solution treatment is presented in Figure 13.

Researchers have examined HA composites with glass reinforcement containing components such as SiO_2 , CaO , MgO , Na_2O , and P_2O_5 . The reason for glass reinforcement is that its chemical content is biocompatible and does not show toxic properties.⁶⁰⁻⁶³ It is an important fact that the content of bioactive glasses contains approximately 60% SiO_2 and a high ratio of $\text{CaO}/\text{P}_2\text{O}_5$. This is because, as this ratio increases, the surface becomes more active in fluid environments like body fluid and blood, and the interactions on the surface increase, then increasing the formation of the HCA layer.

That is, the surface becomes more biocompatible.^{62,63} Phases like calcium phosphate and calcium oxide formed during the formation of the HCA layer are important. For this reason, it is thought that these phases formed as shown in the XRD analysis increased the biocompatibility. TiO_2 peaks were observed in many intervals in the structure before and after the in-vitro treatment. This TiO_2 film formed creates an interface connection between the $\text{Ti}_6\text{Al}_4\text{V}$ base and the HA coating layer.⁵² It was observed that the Al_2O_3 and SiO_2 peaks obtained before the in vitro treatment disappeared after the in-vitro treatment. HA ($\text{Ca}_{10}(\text{PO}_4)_6 \cdot 5(\text{OH})_2$) peak was encountered in the XRD analysis conducted after the in vitro treatment. Four different types of calcium phosphate are used to increase dissolvability: $\text{Ca}_8\text{H}_2(\text{PO}_4)_6 \cdot 5(\text{H}_2\text{O})$, $\text{Ca}_2(\text{PO}_4)_3 \cdot n(\text{H}_2\text{O})$, $\text{Ca}_{10}(\text{PO}_4)_6 \cdot 5(\text{OH})_2$, and $\text{CaHPO}_4 \cdot 2\text{H}_2\text{O}$.⁶⁴ The most intense peak observed after HA was NaOH. The Na^+ ion is the most prevalently found ion in Ringer's solution and human blood plasma.³¹ It is believed that, as Na^+ ions remained on the surface of the specimen kept in Ringer's solution, these provided a peak in the XRD analysis.

FTIR analysis

FTIR analysis was conducted by keeping the B1, B2, and B4 specimens in Ringer's solution for 10 days. The results of the FTIR analysis are shown in Figure 14. In these spectra, it is easy to observe the characteristic absorption bands of HA. O-H bands in the structure of HA are seen at 3750, 630, and 335 cm^{-1} . The characteristic bands of phosphate compounds are encountered within 900 to 1200 and 543 to 601 cm^{-1} . CO_2 stretching bands at 2362 and 2366 cm^{-1} , H_2O stretching bands at 1636 cm^{-1} , and CO_3^{2-} stretching bands at 1458 and 1413 cm^{-1} in the crystal framework structure is observed.⁶⁵⁻⁶⁷ The Ca-PO_4 band is observed at 275 and 295 cm^{-1} , and the Ca-OH band is observed at 335 cm^{-1} . The characteristic bands of HA, PO_4^{3-} groups, are observed at 1090, 14 to 962, 18 to 601, 41 to 473, and 82 to 569 cm^{-1} .⁶⁸⁻⁷¹ It was observed that carbonate groups

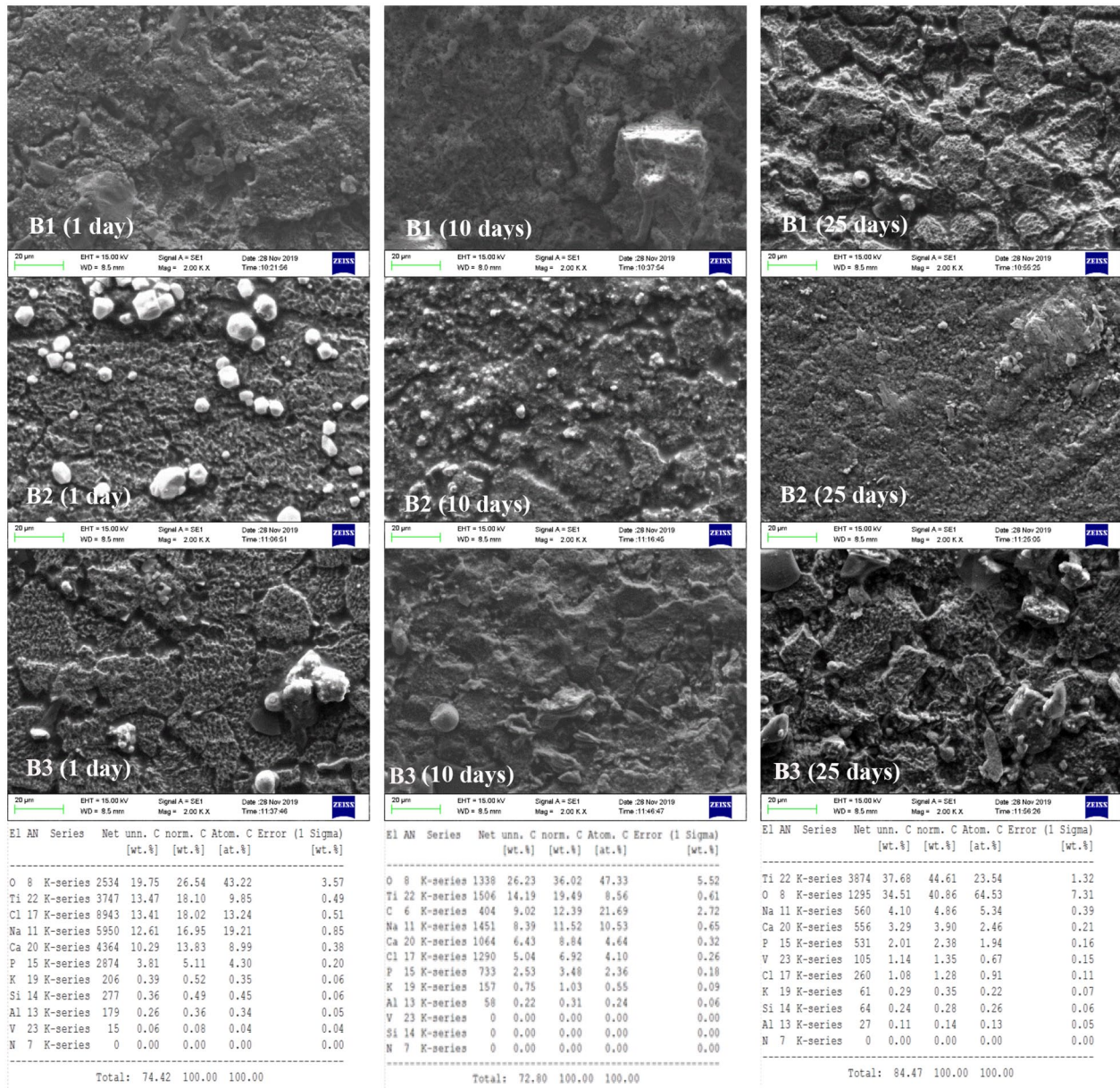


Figure 12. SEM images of affected surfaces of coated samples after in vitro tests in SBF and EDX analysis of B1, B2, and B3 specimens after 10 days.

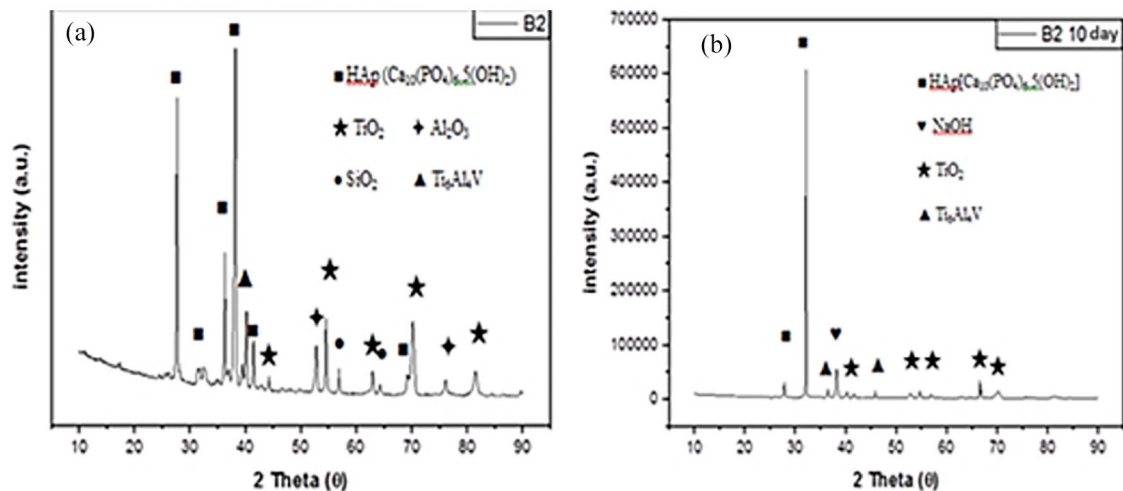


Figure 13. The X-ray diffraction (XRD) pattern of B2 specimen (a) without in vitro (b) with 10 days in vitro treatment.

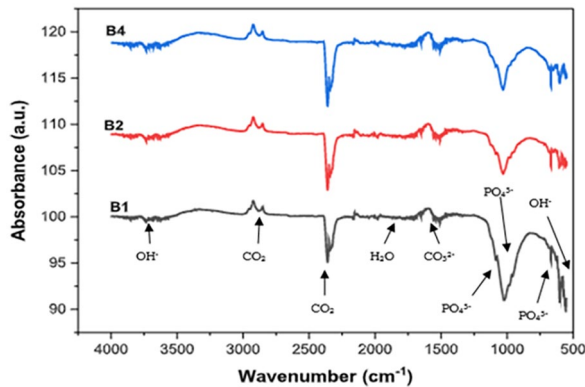


Figure 14. The FTIR spectrum of B1, B2, and B4 specimens.

Table 5. Surface roughness parameters before in vitro and after in vitro for B1, B2, and B3 specimens.

	B1	B2	B4
Before in vitro	Ra: 1237 Rz: 5327 Rq: 1420 Rt: 5390	Ra: 0864 Rz: 2445 Rq: 0,79 Rt: 2609	Ra: 0315 Rz: 0892 Rq: 0363 Rt: 0918
1 day	Ra: 3650 Rz: 10,33 Rq: 3,95 Rt: 10,41	Ra: 0,82 Rz: 2,33 Rq: 0,88 Rt: 2,36	Ra: 5,38 Rz: 15,23 Rq: 6,46 Rt: 15,38
10 days	Ra: 2,94 Rz: 8,33 Rq: 3,06 Rt: 8,41	Ra: 1,25 Rz: 3,53 Rq: 1,27 Rt: 3,57	Ra: 3,99 Rz: 11,29 Rq: 4,64 Rt: 11,4
25 days	Ra: 4,88 Rz: 13,8 Rq: 5,12 Rt: 13,93	Ra: 0,63 Rz: 1,79 Rq: 0,87 Rt: 1,81	Ra: 5,76 Rz: 16,30 Rq: 36,86 Rt: 16,46

were found at 1041 and 598 cm⁻¹, and they formed bone-like apatite structures by solidifying in SBF.⁷² These data were compatible with the study by Lutišanová et al⁷³ conducted with SBF. It is thought that the increase in the peak amplitudes observed in Figure 2 was caused by the increase in the reinforcement components by weight.

Surface roughness results. The pre-in vitro and post-in vitro surface roughness measurements of the coated specimens are given in Table 5. Between the pre- and post-in vitro measurements, it was observed that the surface roughness increased


except for the chitosan-containing specimen. If a biomaterial is rougher, its surface area grows, and the implant adheres better to the surface. Increased surface area also positively affects bone formation.^{36,41,43}

Conclusions

In the scope of this study, it was aimed to coat a hybrid composite (hydroxyapatite/perlite) onto the Ti₆Al₄V implant alloy by using the hydrothermal method. As a result, the following results were observed.

- In the microstructure analysis of the specimens with and without preliminary heat treatment, it was revealed that porous and rough surfaces were formed. It was observed that the surface coatings had an interconnected and porous structure, but no homogenous distribution. Studies have observed that lack of a homogenous distribution on the coating surface makes osteointegration easier. Chitosan provides cell adhesion and multiplication.
- In the specimens without preliminary heat treatment, when the expanded perlite reinforcement ratio is higher than 10 wt.%, it was observed that the coating thickness decreased. In the specimens with preliminary heat treatment, as the expanded perlite reinforcement increased, the coating thickness was observed to increase. The best coating thickness was obtained when the expanded perlite reinforcement ratio are 15 wt.% for specimen with preliminary heat treatment. So; the optimum expanded perlite reinforcement ratio for specimens without preliminary heat treatment is 10 wt.% and it may exceed 15 wt.% for specimens with preliminary heat treatment.
- The result of the XRD analysis showed that the coating formed on the Ti₆Al₄V alloy had a structure of hydroxyapatite and expanded perlite. According to the results of the FTIR analysis, the band intervals formed belonged to the hydroxyapatite and phosphate characteristic bands.
- A hydroxyapatite peak was encountered in the XRD analysis conducted after the in vitro treatment, and it is thought that the layer formation process was going on.
- The increase in the surface roughness values after the in vitro treatment showed that our structure was apatited. With the surface roughness measurements made after the in vitro treatment, it was observed that the surface roughness of the chitosan-containing specimen decreased. Additionally, for the same measurements, it was observed that the surface roughness values increased by an increase in the expanded perlite reinforcement ratio by weight.

ORCID iD

Mehtap Muratoğlu  <https://orcid.org/0000-0002-8237-7869>

REFERENCES

- Von Recum AF. *Handbook of Biomaterials Evolution*. Macmillan; 1986. <https://onlinelibrary.wiley.com/doi/abs/10.1002/jab.770060209>
- Gümüşderelioglu M, Aslankaraoglu E, Gürhan SI. Rabies virus production in non-woven polyester fabric (NWPF) packed-bed reactors. *Appl Biochem*. 2001;33:167-172.
- Park JB, Kim YK. *Metallie Biomaterials, the Biomedical Engineering Handbook*. 2nd ed. CRC Press LLC; 2000.
- Tas AC. Combustion synthesis of calcium phosphate bioceramic powders. *Eur Ceram Soc*. 2000;20:2389-2394.
- Brunette DM, Tenvall P, Textor M, Thomsen P. *Titanium in Medicine*. Springer Verlag; 2001.
- Citeau A, Guicheux J, Vinatier C, et al. In vitro biological effects of titanium rough surface obtained by calcium phosphate grid blasting. *Biomaterials*. 2005;26:157-165.
- Anselme K, Bigerelle M. Topography effects of pure titanium substrates on human osteoblast long-term adhesion. *Acta Biomater*. 2005;1:211-222.
- Yoruc ABH, Karakas A, Gokce H, Buyukpinar C, Karabulut A. Effect of different phosphorus precursors on biomimetic hydroxyapatite powder properties. 2nd International Advances in Applied Physics & Materials Science Congress, Antalya, 2012.
- Anee TK, Ashok M, Palanichamy M, Narayana Kalkura S. A novel technique to synthesize hydroxyapatite at low temperature. *Mater Chem Phys*. 2003;80:725-730.
- Lai W, Chen C, Ren X, Lee IS, Jiang G, Kong X. Hydrothermal fabrication of porous hollow hydroxyapatite microspheres for a drug delivery system. *Mater Sci Eng C*. 2016;62:166-172.
- Albayrak O, Öncel C, Tefek M, Altıntaş S. Effects of calcination on electro-pheretic deposition of naturally derived and chemically synthesized hydroxyapatite. *Rev Adv Mater Sci* 2007;15:10-15.
- Long M, Rack HJ. Titanium alloys in total joint replacement—a materials science perspective. *Biomaterials*. 1998;19:1621-1639.
- Montazeri M, Dehghanian C, Shokouhfar M, Baradaran A. Investigation of the voltage and time effects on the formation of hydroxyapatite-containing titania prepared by plasma electrolytic oxidation on Ti-6Al-4V alloy and its corrosion behavior. *Appl Surf Sci*. 2011;257:7268-7275.
- Durdu S, Deniz ÖF, Kurbay I, Usta M. Characterization and formation of hydroxyapatite on Ti6Al4V coated by plasma electrolytic oxidation. *J Alloys Comp*. 2013;551:422-429.
- Janković A, Eraković S, Vukašinović-Sekulić M, Mišković-Stanković V, Park SJ, Rhee KY. Graphene-based antibacterial composite coatings electrodeposited on titanium for biomedical applications. *Prog Org Coat*. 2015;83:1-10.
- Somiya S, Roy R, Komernani S. *Chemical Processing of Ceramics*. 2nd ed. Taylor & Francis; 2005.
- Jia B, Gao L. Synthesis and characterization of single crystalline PbO nanorods via a facile hydrothermal method. *Mater Chem Phys*. 2006;100:351-354.
- Ilshin Autoclave. Supercritical Hydrothermal Synthesis. Erişim: 31 Mayıs 2012.
- Liu J, Miao X. Sol-gel derived bioglass as a coating material for porous alumina scaffold. *Ceram Int*. 2004;30:1781-1785.
- Vallet-Regí M. Ceramics for medical applications. *J Chem Soc Dalton Trans*. 2001;2:97-108.
- Larry L, Wilson HJ. *An Introduction to Bioceramics*. World Scientific Publishing Co; 1993.
- Sinha A, Ingle A, Munim KR, Vaidya SN, Sharma BP, Bhisey AN. Development of calcium phosphate based bioceramics. *Indian Acad Sci*. 2001;24:653-657.
- Jones JR. Review of bioactive glass: from Hench to hybrids. *Acta Biomaterialia*. 2013;9:4457-4486.
- Deepthi S, Venkatesan J, Kim S-K, Bumgardner JD, Jayakumar R. An overview of chitin or chitosan/nano ceramic composite scaffolds for bone tissue engineering. *Int J Biol Macromol*. 2016;93:1338-1353.
- Li Q, Dunn ET, Grandmaison EW. Applications and properties of chitosan. In: Goosen MFA, ed. *Applications of Chitin and Chitosan*. Technomic Publishing Co.; 1997:3-29.
- Tolga Demirtaş T, Karakeçili AG, Gümüşderelioglu M. Hydroxyapatite containing superporous hydrogel composites: synthesis and in-vitro characterization. *J Mater Sci Mater Med*. 2008;19:729-735.
- González JE, Mirza-Rosca JC. Study of the corrosion behavior of titanium and some of its alloys for biomedical and dental implant applications. *J Electroanal Chem*. 1999;471:109-115.
- Kazek-Kesik A, Krok-Borkowicz M, Dercz G, Donesz-Sikorska A, Pamula E, Simka W. Multilayer coatings formed on titanium alloy surfaces by plasma electrolytic oxidation/electrophoretic deposition methods. *Electrochim Acta*. 2016;204:294-306.
- Sivakumar B, Singh R, Pathak LC. Corrosion behavior of titanium boride composite coating fabricated on commercially pure titanium in Ringer's solution for bioimplant applications. *Mater Sci Eng C*. 2015;48:243-255.
- Fattah-alhosseini A, Ansari AR, Mazaheri Y, Keshavarz MK. Effect of immersion time on the passive and electrochemical response of annealed and nano-grained commercial pure titanium in Ringer's physiological solution at 37°C. *Mater Sci Eng C*. 2017;71:771-779.
- Virtanen S, Milošev I, GomezBarrena E, Trebše R, Salo J, Kontinen YT. Special modes of corrosion under physiological and simulated physiological conditions. *Acta Biomater*. 2008;4:468-476.
- Büyüksağış A. 316 paslanmaz çelik ve Ti6Al4V Alaşımı üzerine Sol Jel Yöntemi ile Hidroksiapatit (HAP) Kaplanması. *Makine Teknolojileri Elektronik Dergisi*. 2010;7:1-11.
- <https://en.perlit.com/expanded-perlite>
- Klawitter JJ, Hulbert SF. Application of porous ceramics for the attachment of load bearing internal orthopedic applications. *J Biomed Mater Res*. 1971;5:161-229.
- Filgueiras MR, LaTorre G, Hench LL. Solution effects on the surface reactions of three bioactive glass compositions. *J Biomed Mater Res*. 1993;27:1485-1493.
- Bobkova NM, Zayats NI, Kolontseva TV, Pun'ko GN, Zakharevich GB. Porous Glass Ceramic Bioimplants. *Glass Ceram*. 2000;57:412-414.
- Thein-Han WW, Misra RD. Biomimetic chitosan-nanohydroxyapatite composite scaffolds for bone tissue engineering. *Acta Biomater*. 2009;5:1182-1197.
- Demirkol N, Nuzhet Oktar F, Sabri Kayali E. Influence of commercial inert glass addition on the mechanical properties of commercial synthetic hydroxyapatite. *Acta Phys Pol A*. 2013;123:427-429.
- Li Z, Ramay HR, Hauch KD, Xiao D, Zhang M. Chitosan-alginate hybrid scaffolds for bone tissue engineering. *Biomaterials*. 2005;26:3919-3928.
- Başpınar MS, Özsoy S, Çolak F, Görhan G, Kara R. Farklı Mineral Yapıya Sahip Kalsiyum Fosfat Tozlarının Sinterlenme Özelliklerinin Karşılaştırılması. *Afyon Kocatepe Üniversitesi Fen Bilimleri Dergisi*. 2009;69-75.
- Murugan R, Ramakrishna S. Development of nanocomposites for bone grafting. *Compos Sci Technol*. 2005;65:2385-2406.
- Say Y, Aksakal B, Dikici B. Effect of hydroxyapatite/sio 2 hyride coatings on surface morphology and corrosion resistance of REX-734 alloy. *Ceram Int*. 2016;42:10151-10158.
- Gross KA, Gross V, Berndt CC. Thermal analysis of amorphous phases in hydroxyapatite coatings. *J Am Ceram Soc*. 2005;81:106-112.
- Shepherd JH, Shepherd DV, Best SM. Substituted hydroxyapatites for bone repair. *J Mater Sci Mater Med*. 2012;23:2335-2347.
- Bang LT, Ishikawa K, Othman R. Effect of silicon and heat treatment temperature on the morphology and mechanical properties of silicon substituted hydroxyapatite. *Ceram Int*. 2011;37:3637-3642.
- Zheng Y, Dong G, Deng C. Effect of silicon content on the surface morphology of silicon-substituted hydroxyapatite bio-ceramics treated by a hydrothermal vapor method. *Ceram Int*. 2014;40:14661-14667.
- Park JB. Biomaterials. In: Bronzino JD, ed. *The Biomedical Engineering Handbook*. 2nd ed. CRC Press LLC; 2000, pp.1-14.
- Rather BD, Hoffman AS. *Biomaterials Science—An Introduction to Materials in Medicine*. 2nd ed. Academic Press; 1996.
- Ratner BD. A history of biomaterials. In: Ratner BD, Hoffman AS, Schoen FJ, Lemons JE, eds. *Biomaterials Science: An Introduction to Materials in Medicine*. 3.baskı ed. Academic Press; 2012;41-53.
- Materials-for-biomedical applications. 2014. <https://ocw.mit.edu/courses/3-051j-materials-for-biomedical-applications-spring>
- Williams DF. On the mechanisms of biocompatibility. *Biomaterials*. 2008;29:2941-2953.
- Nie X, Leyland A, Matthews A. Deposition of layered bioceramic hydroxyapatite/TiO₂ coatings on titanium alloys using a hybrid technique of micro-arc oxidation and electrophoresis. *Surf Coat Technol*. 2000;125:407-414.
- Gür AK, Taşkın M. Metalik Biyomalzemeler ve Biyouyum. 2004;2:106-113.
- Mobasherpour I, Solati Hashjin M, Razavi Toosi SS, Kamachali Darvishi R. Effect of the addition ZrO₂-Al₂O₃ on nanocrystalline hydroxyapatite bending strength and fracture toughness. *Ceram Int*. 2009;35:1569-1574.
- Li P, Ohtsuki C, Kokubo T, et al. Apatite formation induced by silica gel in a simulated body fluid. *J Am Ceram Soc*. 1992;75:2094-2107.
- <http://acikerisim.baskent.edu.tr/handle/11727/6688>
- Pasinli A. Biyomedikal alanlarda kullanılan biyomalzemeler. *Makine Teknolojileri Elektronik Dergisi*. 2004;4:25-34.
- Hench LL, West JK. Biological applications of bioactive glasses. *Life Chem Rep*. 1996;13:187-241.
- Gümüşderelioglu M. *Yeni Ufuklara: Biyomalzemeler*. TÜBİTAK Bilim ve Teknik Dergisi Eki; 2002.

60. Balamurugan A, Balossier G, Kannan S, Rajeswari S. Elaboration of sol-gel derived apatite films on surgical grade stainless steel for biomedical applications. *Mater Lett.* 2006;60:2288.
61. Genc Y, Oktar FN, Erkmen EZ, Göller G, Toykan D, Haybat H. Sintering effect on mechanical properties of enamel derived and synthetic hydroxyapatite-zirconia composites. *Key Eng Mater.* 2004;264-268:1961-1964.
62. Abbasi-Shahni M, Hesarakı S, Behnam-Ghader AA, Hafezi-Ardakani M. Mechanical properties and *in vitro* bioactivity of β -tri calcium phosphate, merwinite nanocomposites. *Key Eng Mater.* 2011;493-494:582-587.
63. Erkmen ZE, Genç Y, Oktar FN. Microstructural and mechanical properties of hydroxyapatite/zirconia Composites. *J Am Ceram Soc.* 2007;90: 2885-2892.
64. Javidi M, Javadpour S, Bahrololoom ME, Ma J. Electrophoretic deposition of natural hydroxyapatite on medical grade 316L stainless steel. *Mater Sci Eng C.* 2008;28:1509-1515.
65. Gören Ş. *Production of Hydroxylapatite from Animal Bone*. Master's thesis. Bogazici University, Bio-Medical Engineering Institute; 2003.
66. Gören Ş, Gökbayrak H, Altıntaş S. Production of hydroxylapatite from animal bone. *Key Eng Mater.* 2004;264-268:1949-1952.
67. Rapacz-Kmita A, Paluszkievicz C, Ślósarczyk A, Paszkiewicz Z. Ftir and XRD investigations on the thermal stability of hydroxyapatite during hot pressing and pressureless sintering processes. *J Mol Struct.* 2005;744-747:653-656.
68. Park J, Lakes RS. *Biomaterials: An Introduction*. 3.baskı ed. Springer; 2007.
69. Kuhn TL. *Biomaterials Introduction to Biomedical Engineering*. 3rd ed. Elsevier Press; 2012.
70. Parkh E, Bronzino D. *The Biomedical Engineering HandBook*. 2nd ed. CRC Press LLC; 2000.
71. Teknoloji Haber Sitesi. Biyomalzemeler, Biyoyuymululuk ve Sınıflandırılması. 2011. <https://dergipark.org.tr/tr/pub/jesd/issue/20871/223984>
72. Ergün Y, Başpınar S, Taktak Ş, Evcin A Titanyum Yüzeyine Sol-Jel Yöntemiyle Hidroksiapatit Kaplanması Afyon Kocatepe Üniversitesi FenVe Mühendislik Bilimleri Dergisi Arşiv Cilt 9, Sayı 3. 2009.
73. Lutišanová G, Kuzielová E, Palou MT, Kozánková J. Static and dynamic in vitro test of bioactivity of glass ceramics. *Ceramics – Silikáty.* 2011;55, 2:106-113.